

# Hysteresis of Finite Arrays of Magnetic Nano Dots.

M. Amin Kayali and Wayne M. Saslow

*Department of Physics, Texas A & M University, College Station, Texas 77843-4242, USA.*

Hysteresis curves for finite arrays of  $N \times N$  ferromagnetic nano dots subject to the dipole-dipole interaction are investigated for  $N = 2 \dots 13$ . Spin arrangements up to  $N = 6$  are presented, which indicate the onset of bulk-like behavior associated with odd ( $N = 5$ ) and even ( $N = 6$ ) systems. The effect of field misalignment on the hysteresis loops is also studied for  $N = 3 \dots 6$ . The area  $A_N$  of the hysteresis loop is studied as a function of  $N$ . We find that  $A_N - A_\infty$  approximately scales as  $N^{-\frac{3}{2}}$  for  $N$  odd and as  $N^{-2}$  for  $N$  even.

PACS numbers: 75.40.Mg; 75.60.Ej; 75.60.Jk; 75.70.Kw

## INTRODUCTION

A ferromagnetic particle goes into a monodomain state if its size  $D$  is below a critical value  $D_c = 10 \sim 100$  nm. This is due to the competition between the exchange and dipolar energies. Therefore, a nanoparticle in a monodomain state may be viewed as a giant magnetic dipole with magnetic moment of thousands of Bohr magnetons. For an  $N \times N$  array of well-separated nanoparticles the exchange energy is usually negligible in comparison with the dipolar and anisotropy and Zeeman energies. The study of such systems is of increasing importance because of their technological applications in data storage devices and magnetic field sensors. As the technology of these devices moves towards higher densities of stored information, it requires smaller particles of magnetic media [1], [2], for which finite size effects become relevant. In finite arrays of such large dipole moment particles, the dipolar field of the array becomes comparable with the bulk anisotropy field. Dipolar effects in such systems affect the static and dynamics properties of the array; and thus must be taken into account.

Recently, Camley and Stamps in [3], [4], [5] investigated the dynamics and magnetization processes of a finite planar array of  $N \times N$  ferromagnetic nano dots, for  $N = 3, 4, 5, 6$ . The nano-dots were taken to interact only via the dipole-dipole interaction, and they were subject to an external field applied either along one side of the array or along its diagonal. They found rather complicated hysteresis loops with the magnetization reversal controlled by the shape anisotropy induced by the array itself. We have considered the same model, and have extended their results, for  $N = 2 \dots 13$ . Our results for  $N = 3$  qualitatively agree with those of [3]. We find that the behavior of these systems is surprisingly complex, both for small and for larger values of  $N$ , and we have studied the approach of these systems to  $N \rightarrow \infty$  behavior.

In the present work each dot is taken to have a radius  $R_d$ , thickness  $d$  and a single degree of freedom corresponding to the orientation of a magnet of saturation magnetization  $M_0$ . We consider only the case of zero

temperature. The dots are arranged on a square lattice with lattice spacing  $a > 2R_d$ , and the dots interact only via the dipole-dipole interaction. The equation of motion for the magnetic moment of each dot is governed by the Landau-Lifshitz-Gilbert equation (LLG), [6] which reads

$$\frac{d\mathbf{M}}{dt} = \gamma \mathbf{M} \times \mathbf{H}_{eff} - \alpha \frac{\mathbf{M} \times (\mathbf{M} \times \mathbf{H}_{eff})}{M_s} \quad (1)$$

where  $\gamma$  is the gyromagnetic ratio,  $\alpha$  is the damping coefficient,  $\mathbf{M}$  is the magnetic moment of the dot and  $M_s = |\mathbf{M}|$  is the saturation magnetization,  $\mathbf{H}_{eff}$  is the average effective magnetic field acting on the dot. The average effective magnetic field acting on the  $i$ -th dot is due to the applied external field, the dipolar fields, and the anisotropy field

$$\mathbf{H}_{eff}^i = H_0 \cos \theta \hat{x} + H_0 \sin \theta \hat{y} - \mathbf{H}_{dip}^i + 2K_1 \frac{m_z^i}{M^2} \hat{z}. \quad (2)$$

Here the dipole field acting on the  $i$ -th dot due to all other dots in the array is given by

$$\mathbf{H}_{dip}^i = \sum_{j \neq i} \frac{\mathbf{M}_j}{r_{ij}^3} - 3 \frac{(\mathbf{M}_j \cdot \mathbf{r}_{ij}) \mathbf{r}_{ij}}{r_{ij}^5} \quad (3)$$

The choice of anisotropy field is determined by the shape of the dot, which in our problem is directed along the symmetry axis of the (cylindrical) dots. We divide both sides of Eq.(1) by  $(\gamma M_s^2)$  and define a dimensionless time variable  $\tau = \gamma M_s t$ . The LLG in these reduced units becomes

$$\frac{d\mathbf{m}}{d\tau} = \mathbf{m} \times \mathbf{h}_{eff} - \frac{\alpha}{\gamma} \mathbf{m} \times (\mathbf{m} \times \mathbf{h}_{eff}) \quad (4)$$

where  $\mathbf{m} = \frac{\mathbf{M}}{M_s}$  and  $\mathbf{h}_{eff} = \frac{\mathbf{H}_{eff}}{M_s}$ . We employ a system of units where magnetic fields are given in units of  $M_s$  and distances are given in units of the array's lattice spacing  $a$ . The strength of the dipole field is characterized by  $h_{dip} = \frac{\pi R_d^2 d}{a^3}$ , which is the ratio of the dot volume to the volume of a cubic cell with side  $a$ . For all arrays studied in this work, we take  $h_{dip} = 0.5$ .

This article is organized as follows. Section II presents the numerical techniques and method of time integration. Section III presents an extensive discussion of magnetization processes and hysteresis for arrays of  $N \times N$  nano dots ( $N = 2, 3, \dots, 13$ ) when the external field is applied along one side of the array. Section IV considers the effects on the hysteresis loop of misalignment of the external field. Section V considers the relationship between the area of the hysteresis loop and  $N$ . A brief summary is given in section VI.

## NUMERICAL TECHNIQUES

We have employed two different approaches to study the magnetization processes of our  $N \times N$  arrays of nano-dots. The first approach uses the second rank Runge-Kutta (RK) algorithm with fixed time step to integrate the LLG equation in reduced units. The second approach uses the ‘‘greedy algorithm’’ to find the stable final state of the array. In both approaches the calculations were done using FORTRAN and Mathematica languages [7]. The two approaches yielded similar results.

In the RK approach, the integration is done using a fixed time step  $\Delta\tau = 5 \times 10^{-3}$  and a damping coefficient  $\frac{\alpha}{\gamma} = 0.6$ , with an initial state in which the magnetic moment of the dot is randomly generated. The time integration proceeds until a stable final state is reached. The stability of the final state is checked by changes in the total energy of the system. Iterations are stopped when the difference between the total energy of the system from the  $(n+1)$ -th iteration and that of the  $n$ -th iteration is of the order of  $\Delta E_n = 10^{-5}$  in units of  $M_s^2 a^3$ . Our solutions converged after almost  $10^3$  iterations.

The greedy algorithm approach assumes the dots to be aligned along the direction of their total local field. In the initial state each dot is chosen to point randomly. Next, all components of the total local field are calculated for each dot. Finally each component of the field is normalized by the magnitude of the total local field to yield the new dot magnetization orientation. The final state of the  $n$ -th iteration is used as an initial one for the next iteration until the solution is converged. The convergence of the final state is checked in manner similar to that used in the first approach. Note that the greedy algorithm can be obtained from the LLG equation in the limit where the damping coefficient is very large. We find that the LLG approach converges faster than the greedy algorithm. This is probably related to a phenomenon known in RLC circuits, where a critically-damped circuit approaches equilibrium faster than a circuit with a larger amount of damping.

Calculation of the dipolar field at the  $i$ -th dot is the most computationally time-consuming aspect of both approaches since it requires summation of the dipole fields from all other dots in the array. However, due to the

relatively small sizes of our dot arrays this calculation is performed rather quickly.

## HYSTERESIS LOOP AND EXTERNAL FIELD ORIENTATION EFFECT

Hysteresis loops  $M(H)$  for  $N \times N$  arrays of nano dots subject to an external magnetic field applied along one side have been calculated. Initially, a strong external field  $H_0$  is applied to the array until saturation. Then the field is decreased to  $-H_0$ , and then is increased again up to  $H_0$ . We have taken  $H_0 = 2M_s$ , and a fixed field-step of  $\Delta H = 2 \times 10^{-3}M_s$  is used to simulate the sweeping process. For each value of the external field the system was iterated until a stable final state is reached. As seen in Fig. 1, where  $M(H)$  is plotted (both in units of  $M_s$ ), the odd and even  $N$  arrays have somewhat different behaviors, especially for small  $N$ . One aspect of this is that the odd- $N$  systems display magnetization jumps as the field changes. The odd- $N$  and even- $N$  behavior becomes similar for larger values of  $N$ , something we study in a later section.

In Fig. 1, the angle of the field to one of the sides (the  $y$ -axis) is taken to be  $\theta = 0$ . Experimentally, however, field misalignment is almost inevitable, so that we have also studied this phenomenon.

Fig. 2 shows results for  $N = 3 \dots 6$  and angles  $\theta = 5^\circ, 30^\circ$ , and  $45^\circ$ . (We present only some of the more representative results; angles between 0 and  $45^\circ$  were studied in  $5^\circ$  increments.)

Comparison of Fig. 1 with Fig. 2 for  $\theta = 5^\circ$  shows that a small misalignment of the applied field can change the hysteresis loop drastically.

For  $N = 3$ , Fig.2 shows that the central part of the hysteresis loop shrinks as  $\theta$  increases. For  $\theta = 45^\circ$ , the central part almost disappears completely, and new small loops start to develop away from the center of the hysteresis loop. Our results for  $N = 3$  agree with those given in [3], which studied the cases  $\theta = 0^\circ$  and  $45^\circ$ .

For  $N = 4$ , at  $\theta = 0^\circ$  there is no central loop, but there is a prominent loop at finite field. On the other hand, at  $\theta = 5^\circ$ , there is a central loop, and the finite field structure becomes rather complex. Further increase of  $\theta$  leads to a filling out and connecting of various subloops. Also, note the appearance of jumps for non-zero  $\theta$ .

For  $N = 5$ , a small field misalignment has an enormous effect, at  $\theta = 5^\circ$  shrinking the loop to a relatively small central region. As  $\theta$  increases, the central loop grows, but the loop for  $\theta = 45^\circ$  pinches off to yield three subloops, as for  $N = 3$ .

For  $N = 6$ , again a small field misalignment has an enormous effect, at  $\theta = 5^\circ$  shrinking the loop to a relatively small central region. As  $\theta$  increases, the central loop grows, but in contrast to  $N = 5$ , the loop for  $\theta = 45^\circ$  does not pinch off, and closely resembles the loop for

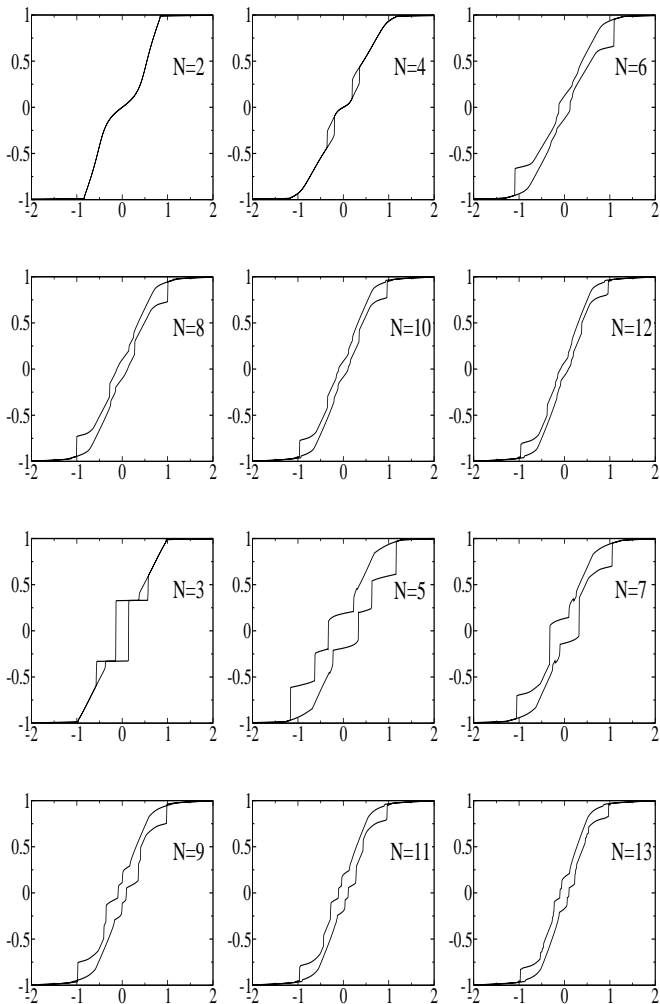


FIG. 1: Hysteresis loops  $M(H)$ , both in units of  $M_s$ , for weakly coupled arrays of  $N \times N$  ferromagnetic nano dots. The external field is applied along the  $y$ -axis, which coincides with one side of the array. The top two rows are for  $N$  even and the lower two are for  $N$  odd.

$N = 4$ .

These different types of behavior indicates that these are complex systems, for which it is difficult to make generalizations.

### HYSTERESIS AND EVEN-ODD SIGNATURE IN FINITE ARRAY OF NANO-DOTS

In the absence of an external magnetic field the array of  $N \times N$  nano-dots favors antiferromagnetic ordering, thus minimizing its magnetostatic energy. A large external magnetic field applied to the array tends to orient the magnetic moments along the field, thus minimizing the Zeeman field energy. However, the spins at the array corners tip by a small angle, as shown in Fig. 3-Fig. 6, forming a two-dimensional “flower” state [8], [9]. The flower state persists until the applied field falls to  $H_0 = M_s$ . For

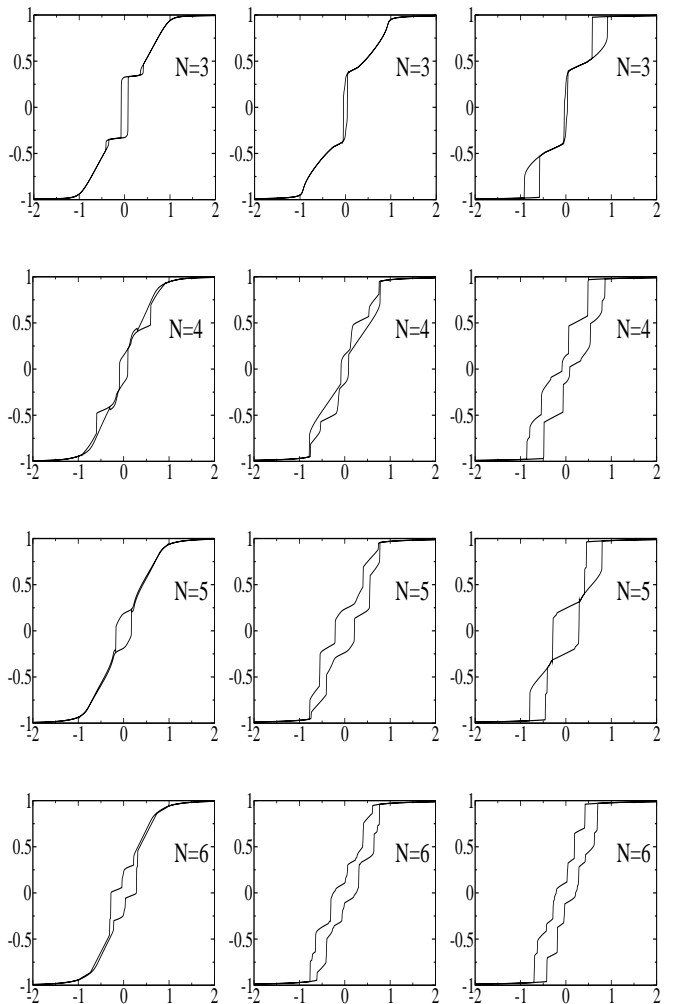


FIG. 2: Hysteresis loops  $M(H)$ , both in units of  $M_s$ , for  $N = 3 \dots 6$  arrays for the field at  $\theta = 5^\circ, 30^\circ$  and  $45^\circ$  going from left to right.

lower values of the applied field, the competition between the dipole-dipole interaction and the Zeeman energy becomes significant, and changes the array ordering.

For  $N = 2$ , Fig. 3 shows that below  $H_0 = M_s$  and for  $H_0 \neq 0$  the spins form a snake-like domain structure winding clockwise or counterclockwise. At  $H_0 = 0$ , the array has zero net per-dot magnetization, due to a vortex-like structure that persists for  $-3M_s \leq H_0 \leq 0.3M_s$ .

The  $N = 3$  array was analysed by Camley and Stamps in [3]. This array also shows snake-like arrangements below  $H_0 = M_s$ . At zero field the final state of the array shows what we call a “barrel” state in which the spins at the left and right columns are oriented opposite to the central column with a slight tipping of the corner spins, as shown in Fig. 4. This agrees with Ref. 3 except for the tipping of the corner spins. We have made a small angle expansion of the energy for the spins being nearly aligned, and indeed we find that the tipped corner spin state is more energy favorable. The tipping angle was determined

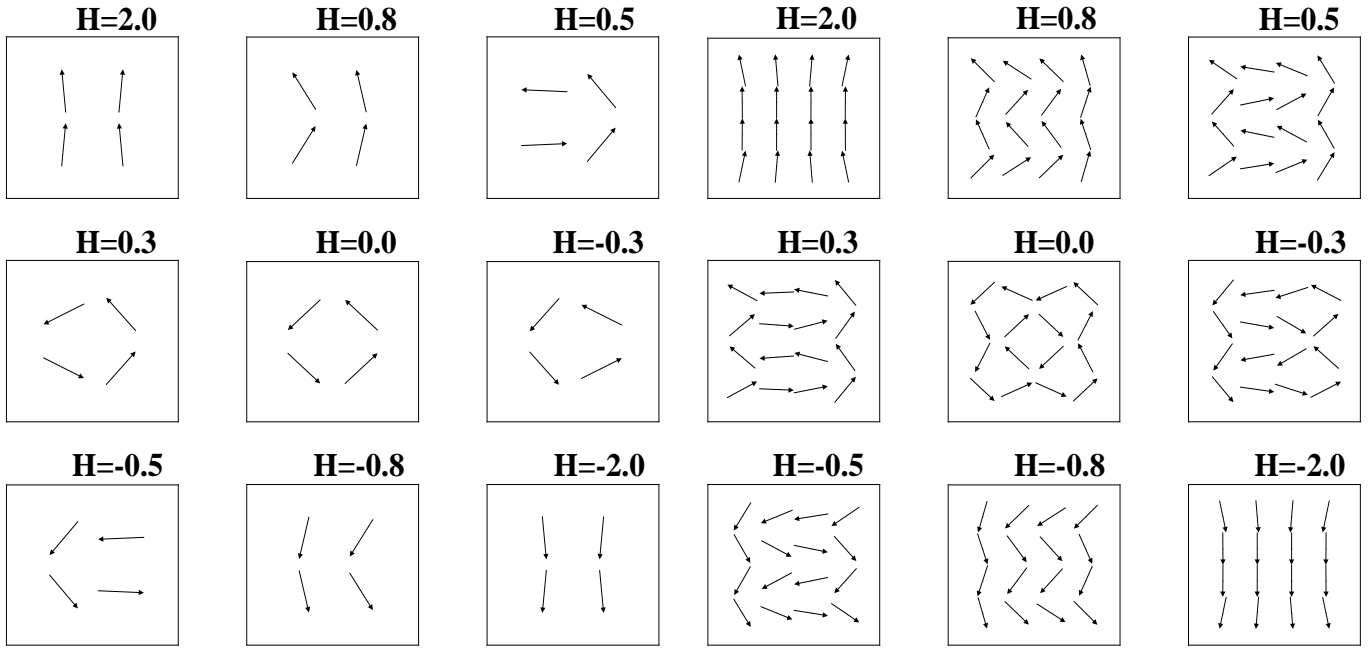


FIG. 3: Spin arrangements for an array of  $2 \times 2$  ferromagnetic nano dots in external magnetic field.

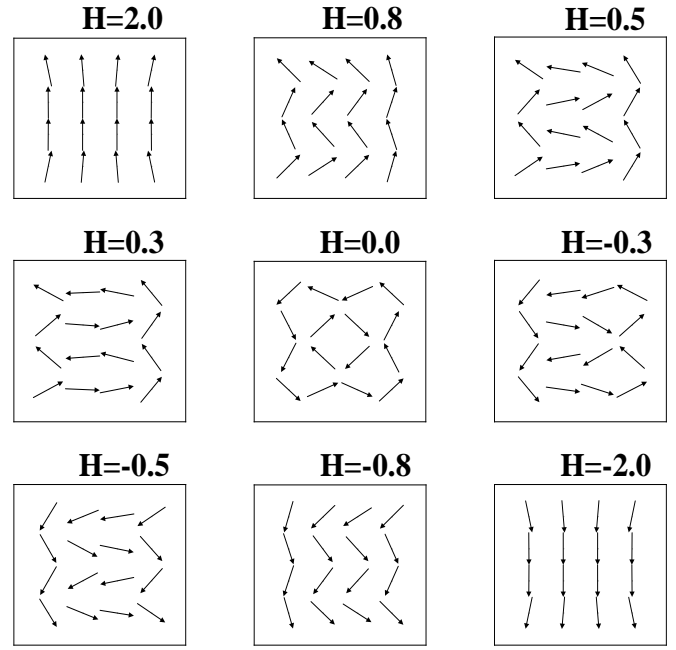


FIG. 5: Spin arrangements for an array of  $4 \times 4$  ferromagnetic nano dots in external magnetic field.

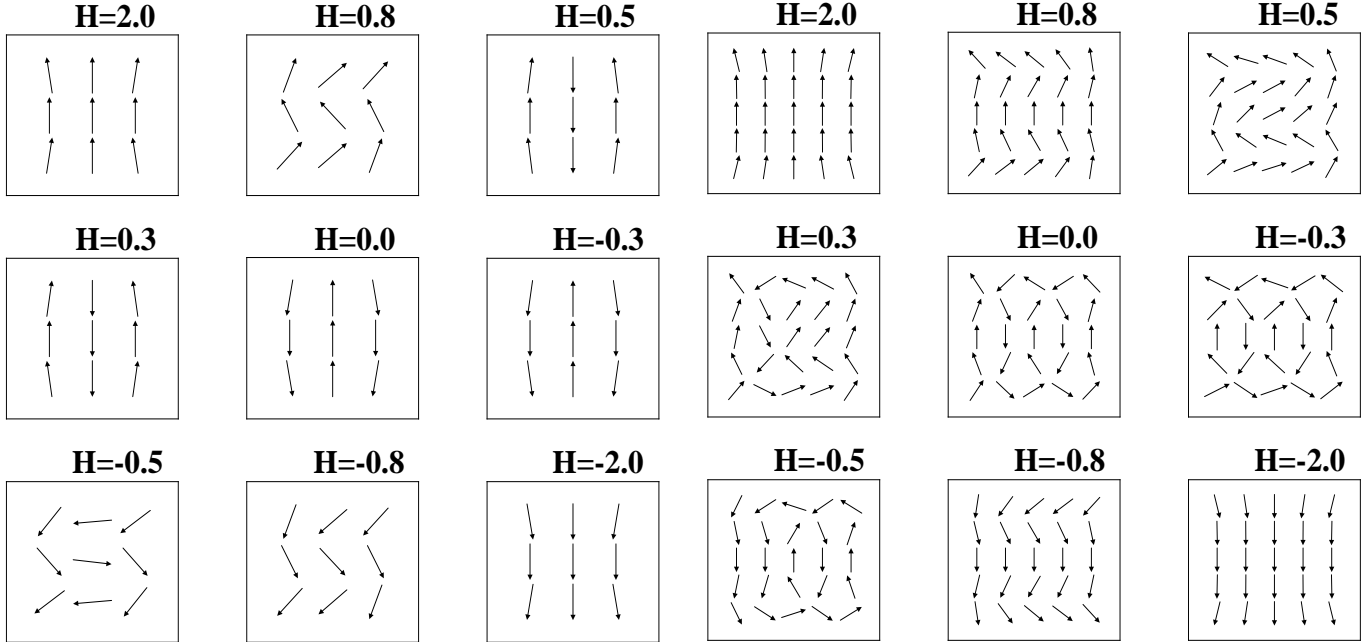


FIG. 4: Spin arrangements for an array of  $3 \times 3$  ferromagnetic nano dots in an external magnetic field.

FIG. 6: Spin arrangements for an array of  $5 \times 5$  ferromagnetic nano dots in external magnetic field.

by both iteration and analytical calculations, and agreement is found between the two values. The numerical value of the corner spin tipping angle, found both by iteration and small tipping angle analysis, is  $|\alpha| = 9.1115^\circ$ , with numerical error of order  $10^{-5}$ . The spin snapshots in Fig. 4 and hysteresis loop analysis show that the barrel state switches to an inverted barrel state when the

applied field changes sign.

Fig.5 shows that the  $N = 4$  array also features snake-like arrangements of the spins, for intermediate values of the applied field. However, in zero field the total per-dot magnetization is zero, which can be attributed to the formation of a vortex in the array's central  $2 \times 2$  block. The magnetic moments of the rest of the dots

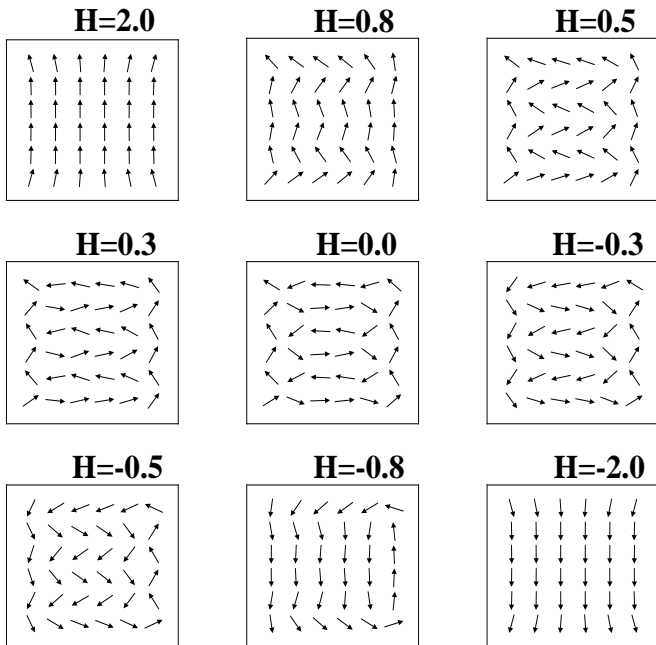


FIG. 7: Spin arrangements for an array of  $6 \times 6$  ferromagnetic nano dots in external magnetic field.

in the array form a ring that surrounds the vortex with opposite circulation. This state is stable for applied fields  $H_0$  satisfying  $-0.2M_s \leq H_0 \leq 0.2M_s$ .

For all  $N$ , the flower state appear at high fields (here,  $|H_0| = 2.0M_s$ ). The hysteresis loops shown in Fig. 1 show a subtle difference in shape between arrays with odd  $N$  and arrays with even  $N$ . For odd  $N$  the loops show well-defined jumps whereas for even  $N$  this behavior is absent. This behavior is due to unpaired spins with uncompensated dipole fields. The jumps become less apparent as  $N$  grows, and will eventually disappear for large  $N$ , where the distinction between even and odd  $N$  becomes unimportant.

Note that, when an array was placed in zero external field and given random initial conditions, the solutions converged to the same states as obtained in the hysteresis-cycle calculations, up to the degeneracy of the system. Thus, for  $N = 2, 4$  there are two degenerate metastable states of opposite chirality (winding) with zero net magnetization in zero field, each of which has a four-fold rotational symmetry. For  $N = 6$  there are two degenerate states of opposite chirality, with non-vanishing net magnetization, each of these state has no apparent rotational symmetry. For  $N = 3$  there are two degenerate barrel states, with no rotational symmetry, and  $N = 5$  is similar to  $N = 6$ . The hysteresis loop area  $A_N$  will produce further evidence that large system behavior commences with  $N = 5$  and  $N = 6$ . Metastable states with vanishing net magnetization may appear for arrays with even  $N$ . However, our simulations showed that these states could appear only for  $N = 2, 4$ . For

arrays with odd  $N$  the unpaired dipoles prevent the formation of such states.

### HYSTERESIS LOOP AREA $A_N$ VS. PARTICLE NUMBER $N$

Although the area of the hysteresis loop  $A_N$  tends to zero for the  $N = 2$  array, it clearly is nonzero for all other arrays. We present the hysteresis loop areas in Fig. 8 as circles and squares. From Fig. 8, we see that the area of the hysteresis loop decreases with increasing  $N$  except for  $N = 3$  for  $N$  odd and  $N = 2, 4$  for  $N$  even. The  $N = 5$  and  $N = 6$  arrays, the first to show something like bulk behavior, have maximum  $A_N$  for odd and even respectively; their spin arrangements are given in Fig. 6 and Fig. 7. We have fitted our data to the asymptotic form

$$A_N = A_\infty + \frac{C}{N^p} \quad (5)$$

where  $A_\infty$ ,  $C$  and  $p$  are constants to be determined. If larger values of  $N$  had been computationally feasible, we would have considered only large values of  $N$  for the fit. The fit is not as good when  $N = 5$  is included, so we do not show this case. In practice, for  $N$  odd the data are fit starting from  $N = 7$  and for  $N$  even from  $N = 6$ . Both fits are shown as solid lines in Fig. 8, where the values of  $A_\infty$ ,  $C$ , and  $p$  are given in the table.

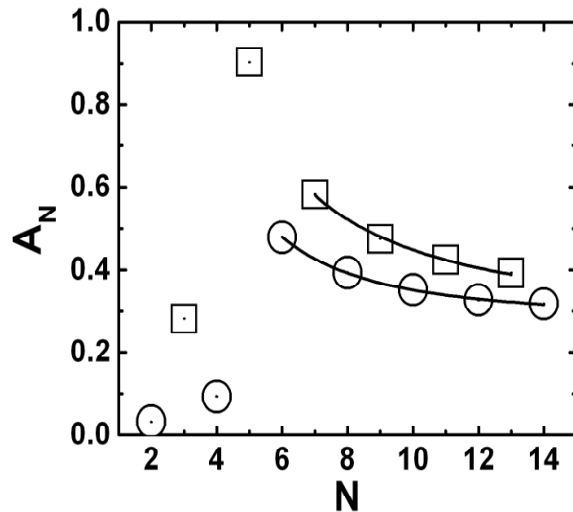


FIG. 8: The area of the hysteresis loop as a function of the number of particles  $N$ .

The associated values of  $\chi^2$  are both less than  $10^{-5}$ . For odd  $N$ ,  $A_N$  varies approximately as  $A_N \sim N^{-\frac{3}{2}}$  whereas for even  $N$  it varies approximately as  $N^{-2}$ . We attribute no fundamental significance to these values.

TABLE I: Fitting parameters for data given in Fig. 8, using Eq. 5.

N	$A_\infty$	$C$	$p$
even	0.278	$6.31 \pm 0.42$	$1.95 \pm 0.03$
odd	0.278	$6.92 \pm 0.86$	$1.61 \pm 0.06$

### SUMMARY

We have studied the hysteresis and magnetization processes for  $N \times N$  arrays (with  $N = 2 \dots 13$ ) of uniaxial ferromagnetic nano dots interacting via the dipole-dipole interaction. For an external magnetic field aligned or misaligned with one side of the array, the hysteresis loops are surprisingly complex. For arrays with odd  $N$  the hysteresis loops possess jumps, whereas for even  $N$  they do not. As  $N$  increases, the area  $A_N$  of the hysteresis loop begins to saturate, approaching a non-zero finite value determined from a data fit. The area of the hysteresis loop scales with  $N$  approximately as  $N^{-\frac{3}{2}}$  for  $N$  odd, and approximately as  $N^{-2}$  for even.

We would like to thank V. L. Pokrovsky, A. S. Kirakosyan and S. Erdin for fruitful discussions. This work was supported by NSF grants DMR 0103455 and

DMR 0072115, DOE grant DE-FG03-96ER45598, and Telecommunication and Information Task Force at Texas A&M University.

- 
- [1] E. C. Stoner and E. P. Wohlfarth, *Philos. Trans. R. Soc. London, Ser. A* **240**, 599(1948).
  - [2] J. F. Smyth, S. Schultz, D.R. Fradkin, *et.al.*, *J. Appl. Phys.* **69**, 5262 (1991).
  - [3] R. L. Stamps and R. E. Camley, *Phys. Rev.* **B60**, 11694 (1999).
  - [4] R. L. Stamps and R. E. Camley, *Phys. Rev.* **B60**, 12264 (1999).
  - [5] R. L. Stamps and R. E. Camley, *J. Magn. Magn. Mater.* **177-181**, 813 (1998).
  - [6] E. M. Lifshitz and L. P. Pitaevskii, *Course of Theoretical Physics* Vol. 5: *Statistical Physics* (Pergamon, New York, 1980), Part 2.
  - [7] S. Wolfram, *The Mathematica Book*, Cambridge University Press, (Cambridge, 2002).
  - [8] A. Aharoni, *Introduction to the Theory of Ferromagnetism*, Oxford Univ. Press, (Oxford, 2001).
  - [9] V. Ternovsky, B. Luk'yanchuk and J. P. Wang, *Pis'ma Zh. Eksp. Teor. Fiz.* **73**, 746 (2001)[*JETP Lett.* **73**,661 (2001)].